

Adaptive discontinuous Galerkin methods for non-linear diffusion-convection-reaction equations

Murat Uzunca^{a,*}, Bülent Karasözen^b, Murat Manguoğlu^c

^aDepartment of Mathematics, Middle East Technical University, 06800 Ankara, Turkey

^bDepartment of Mathematics and Institute of Applied Mathematics, Middle East Technical University, 06800 Ankara, Turkey

^cDepartment of Computer Engineering and Institute of Applied Mathematics, Middle East Technical University, 06800 Ankara, Turkey

Abstract

In this work, we apply the adaptive discontinuous Galerkin (DGAFEM) method to the convection dominated non-linear, quasi-stationary diffusion-convection-reaction equations. We propose an efficient preconditioner using a matrix reordering scheme to solve the sparse linear systems iteratively arising from the discretized non-linear equations. Numerical examples demonstrate effectiveness of the DGAFEM to damp the spurious oscillations and resolve well the sharp layers occurring in convection dominated non-linear equations.

Keywords: non-linear diffusion-convection reaction, discontinuous Galerkin, adaptivity, matrix reordering, preconditioning

1. Introduction

Many engineering problems such as chemical reaction processes, heat conduction, nuclear reactors, population dynamics etc. are governed by coupled convection-diffusion-reaction partial differential equations (PDEs) with non-linear source or sink terms. It is a significant challenge to solve such PDEs numerically when they are convection/reaction-dominated. As a model problem, we consider the coupled quasi-stationary equations arising from the time discretization of time-dependent non-linear diffusion-convection-reaction equations (Bause & Schwegler, 2012)

$$\alpha u_i - \epsilon_i \Delta u_i + \mathbf{b}_i \cdot \nabla u_i + r_i(\mathbf{u}) = f_i \quad \text{in } \Omega_i, \quad (1a)$$

$$u_i = g_i^D \quad \text{on } \Gamma_i^D, \quad (1b)$$

$$\epsilon_i \nabla u_i \cdot \mathbf{n} = g_i^N \quad \text{on } \Gamma_i^N, \quad i = 1, \dots, m \quad (1c)$$

with Ω_i are bounded, open, convex domains in \mathbb{R}^2 with boundaries $\partial\Omega_i = \Gamma_i^D \cup \Gamma_i^N$, $\Gamma_i^D \cap \Gamma_i^N = \emptyset$, $0 < \epsilon_i \ll 1$ are the diffusivity constants, $f_i \in L^2(\Omega)$ are the source functions, $\mathbf{b}_i \in (W^{1,\infty}(\Omega))^2$ are

*Corresponding author. Tel.: +90 312 2105353.

Email addresses: uzunca@metu.edu.tr (Murat Uzunca), bulent@metu.edu.tr (Bülent Karasözen), manguoglu@ceng.metu.edu.tr (Murat Manguoğlu)

Preprint submitted to Elsevier

September 16, 2014

the velocity fields, $g_i^D \in H^{3/2}(\Gamma_i^D)$ are the Dirichlet boundary conditions, $g_i^N \in H^{1/2}(\Gamma_i^N)$ are the Neumann boundary conditions, and $\mathbf{u}(x) = (u_1, \dots, u_m)^T$ and \mathbf{n} denote the vector of unknowns and normal vector to the boundary, respectively. The coefficients of the linear reaction terms, $\alpha > 0$, stand for the temporal discretization, corresponding to $1/\Delta t$, where Δt is the discrete time-step. Moreover, we assume that the non-linear reaction terms are bounded, locally Lipschitz continuous and monotone, i.e. satisfy for any $s, s_1, s_2 \geq 0$, $s, s_1, s_2 \in \mathbb{R}$ the following conditions (Bause & Schwegler, 2012)

$$|r_i(s)| \leq C, \quad C > 0 \quad (2a)$$

$$\|r_i(s_1) - r_i(s_2)\|_{L^2(\Omega)} \leq L\|s_1 - s_2\|_{L^2(\Omega)}, \quad L > 0 \quad (2b)$$

$$r_i \in C^1(\mathbb{R}_0^+), \quad r_i(0) = 0, \quad r'_i(s) \geq 0. \quad (2c)$$

The non-linear reaction terms $r_i(\mathbf{u})$ occur in chemical engineering usually in the form of products and rational functions of concentrations, or exponential functions of the temperature, expressed by the Arrhenius law. Such models describe chemical processes and they are strongly coupled as an inaccuracy in one unknown affects all the others. Hence, efficient numerical approximation of these systems is needed. For the convection/reaction-dominated problems, the standard Galerkin finite element methods are known to produce spurious oscillations, especially in the presence of sharp fronts in the solution, on boundary and interior layers.

In last two decades several stabilization and shock/discontinuity capturing techniques were developed for linear and non-linear stationary and time dependent problems. For linear convection dominated problems, the streamline upwind Petrov-Galerkin(SUPG) method is capable to stabilize the unphysical oscillations (Bause, 2010; Bause & Schwegler, 2012, 2013). Nevertheless, in non-linear convection dominated problems, spurious oscillations are still present in crosswind direction. Therefore, SUPG is used with the anisotropic shock capturing technique as SUPG-SC for reactive transport problems (Bause, 2010; Bause & Schwegler, 2012, 2013). It was shown that SUPG-SC is capable of reducing the unphysical oscillations in cross-wind direction. The parameters of the SUPG and SUPG-SC should be designed carefully for the efficient solution of the discretized equations.

In contrast to the standard Galerkin conforming finite element methods, discontinuous Galerkin finite element(DGFEM) methods produce stable discretizations without the need for stabilization strategies, and damp the unphysical oscillations for linear convection dominated problems. In (Yücel et al., 2013), several non-linear convection dominated problems of type (1) are solved with DG-SC, discontinuous Galerkin method with the shock-capturing technique in (Persson & Peraire, 2006). For an accurate solution of non-linear convection dominated problems, higher order finite elements are used because they are less diffusive and avoid artificial mixing of chemical species under discretization, for SUPG-SC and DG-SC, respectively. The main advantages of DGFEM are the flexibility in handling non-matching grids and in designing hp-refinement strategies (Houston et al., 2002), which allow easily adaptive grid refinement. In this paper we extend the adaptive discontinuous Galerkin method in (Schötzau & Zhu, 2009) to the convection dominated non-linear problems of type (1). We show on several examples the effectiveness and accuracy of DGAFEM capturing boundary and internal layers very sharply and without significant oscillations. An important drawback is that the resulting linear systems are more dense than the continuous finite elements and ill-conditioned. The condition number grows rapidly with the number of elements and with the penalty parameter. Therefore, efficient solution strategies such as preconditioning are required to solve the linear systems. While more robust compared to iterative solvers, direct solvers are usually more memory and time consuming due to fill-in.

Furthermore, they are known to be less scalable on parallel architectures. Therefore, in this paper we use an iterative method which is robust and efficient.

Because the DG method requires more degrees of freedom than the standard Galerkin method, in (Cangiani et al., 2103) linear diffusion-convection-reaction equations are discretized near the boundary and inter layers by the interior penalty DG method, away from the layers by continuous Galerkin method. It was shown that combination of both methods will not affect the stability of the DG method. Another important class of non-linear diffusion-convection equations are those with the non-linear convective term, including the viscous Burger's equation. In the recent years, several effective interior penalty DG methods with efficient time integrators and with space and time adaptivity for this class of problems are developed, see for example (Dolejši, 2008; Dolejši et al., 2005; Dolejši, 2013). An important class of non-linear convection-diffusion equations are the pellet equations, which model the intra-particle mass and heat transport in porous catalyst pellets. A comprehensive review of weighted residual methods, the orthogonal collocation, Galerkin, tau and least squares methods is given in (Solsvik et al., 2013) for solving the linear and non-linear pellet equations, where the methods are compared with respect to convergence of the residuals and computational efficiency.

The rest of this work is organized as follows. In the next two sections, we give the DG discretization and describe the residual based adaptivity for non-linear diffusion-convection-reaction problems. In Section 4, we have compared the DGFEM and DGAFEM with another class of stabilized methods, the GLSFEM (Galerkin least square finite element method) for a linear convection dominated problem. Section 5 deals with an efficient solution technique for solving the linear system arising from the DG discretization. In Section 6, we demonstrate the effectiveness and accuracy of DGAFEM for handling the sharp layers arising in several examples with different type of non-linear reaction mechanisms. The paper ends with some conclusions.

2. Symmetric discontinuous interior penalty Galerkin (SIPG) discretization

In this Section, we describe the DG discretization of the model problem (1). We begin with the classical weak formulation of the scalar equation ($m = 1$) of (1): find $u \in U$ such that

$$\int_{\Omega} (\epsilon \nabla u \cdot \nabla v + \mathbf{b} \cdot \nabla uv + \alpha uv) dx + \int_{\Omega} r(u) v dx = \int_{\Omega} f v dx + \int_{\Gamma^N} g^N v ds, \quad \forall v \in V \quad (3)$$

where the solution space U and the test function space V are given by

$$U = \{u \in H^1(\Omega) : u = g^D \text{ on } \Gamma^D\}, \quad V = \{v \in H^1(\Omega) : v = 0 \text{ on } \Gamma^D\}.$$

Under the assumptions given in the previous section, the problem (3) has a unique solution in U . The next step of the classical (continuous) FEM is to find an approximation to the problem (3) using a conforming, finite-dimensional subspace $V_h \subset V$, which requires that the space V_h contains functions of particular smoothness (e.g. when $V = H_0^1(\Omega)$, then we choose $V_h \subset \{v \in C(\bar{\Omega}) : v = 0 \text{ on } \partial\Omega\}$). On the other hands, discontinuous Galerkin methods make it easy to use the non-conforming spaces, in which case the functions in $V_h \not\subset V$ are allowed to be discontinuous on the inter-element boundaries.

In this article, the discretization of the problem (1) is based on the symmetric discontinuous interior penalty Galerkin (SIPG) method, a type of discontinuous Galerkin methods, for the

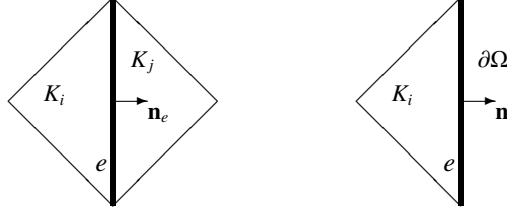


Figure 1: Two adjacent elements sharing an edge (left); an element near to domain boundary (right)

diffusion part (Arnold et al., 2002; Rivière, 2008) and the upwinding for the convection part (Ayuso & Marini, 2009; Houston et al., 2002).

Let $\{\xi_h\}$ be a family of shape regular meshes with the elements (triangles) $K_i \in \xi_h$ satisfying $\overline{\Omega} = \cup \overline{K}$ and $K_i \cap K_j = \emptyset$ for $K_i, K_j \in \xi_h$. Let us denote by Γ^0 , Γ^D and Γ^N the set of interior, Dirichlet boundary and Neumann boundary edges, respectively, so that $\Gamma^0 \cup \Gamma^D \cup \Gamma^N$ forms the skeleton of the mesh. For any $K \in \xi_h$, let $\mathbb{P}_k(K)$ be the set of all polynomials of degree at most k on K . Then, set the finite dimensional solution and test function space by

$$V_h = \{v \in L^2(\Omega) : v|_K \in \mathbb{P}_k(K), \forall K \in \xi_h\} \not\subset V.$$

Note that the trial and test function spaces are the same because the boundary conditions in discontinuous Galerkin methods are imposed in a weak manner (see the SIPG construction below). Since the functions in V_h may have discontinuities along the inter-element boundaries, along an interior edge, there would be two different traces from the adjacent elements sharing that edge. In the light of this fact, let us first introduce some notations before starting the construction of SIPG formulation. Let $K_i, K_j \in \xi_h$ ($i < j$) be two adjacent elements sharing an interior edge $e = K_i \cap K_j \subset \Gamma_0$ (see Fig.1). Denote the trace of a scalar function v from inside K_i by v_i and from inside K_j by v_j . Then, set the jump and average values of v on the edge e

$$[v] = v_i \mathbf{n}_e - v_j \mathbf{n}_e, \quad \{v\} = \frac{1}{2}(v_i + v_j),$$

where \mathbf{n}_e is the unit normal to the edge e oriented from K_i to K_j . Similarly, we set the jump and average values of a vector valued function \mathbf{q} on e

$$[\mathbf{q}] = \mathbf{q}_i \cdot \mathbf{n}_e - \mathbf{q}_j \cdot \mathbf{n}_e, \quad \{\mathbf{q}\} = \frac{1}{2}(\mathbf{q}_i + \mathbf{q}_j),$$

Observe that $[v]$ is a vector for a scalar function v , while, $[\mathbf{q}]$ is scalar for a vector valued function \mathbf{q} . On the other hands, along any boundary edge $e = K_i \cap \partial\Omega$, we set

$$[v] = v_i \mathbf{n}, \quad \{v\} = v_i, \quad [\mathbf{q}] = \mathbf{q}_i \cdot \mathbf{n}, \quad \{\mathbf{q}\} = \mathbf{q}_i$$

where \mathbf{n} is the unit outward normal to the boundary at e .

Now, we are ready to construct the SIPG discretization of the diffusion part of the problem. We start with the continuous (i.e. assume for the moment that the unknown solution u is smooth enough) Poisson problem

$$-\Delta u = f \quad \text{in } \Omega, \tag{4a}$$

$$u = g^D \quad \text{on } \Gamma^D \tag{4b}$$

$$\nabla u \cdot \mathbf{n} = g^N \quad \text{on } \Gamma^N \tag{4c}$$

We multiply the equation (4a) by a test function $v \in V_h$, we integrate over Ω and we split the integrals:

$$-\sum_{K \in \xi_h} \int_K \Delta u v dx = \sum_{K \in \xi_h} \int_K f v dx$$

Apply the divergence theorem on every element integral

$$\sum_{K \in \xi_h} \int_K \nabla u \cdot \nabla v dx - \sum_{K \in \xi_h} \int_{\partial K} (\nabla u \cdot \mathbf{n}) v ds = \sum_{K \in \xi_h} \int_K f v dx + \sum_{e \in \Gamma_N} \int_e g^N v ds$$

Or using the jump definitions ($v \in V_h$ are element-wise discontinuous)

$$\sum_{K \in \xi_h} \int_K \nabla u \cdot \nabla v dx - \sum_{e \in \Gamma_0 \cup \Gamma^D} \int_e [v \nabla u] ds = \sum_{K \in \xi_h} \int_K f v dx + \sum_{e \in \Gamma_N} \int_e g^N v ds$$

One can easily verify that $[v \nabla u] = \{\nabla u\} \cdot [v] + [\nabla u] \cdot \{v\}$. Then, using also the fact that $[\nabla u] = 0$ (u is assumed to be smooth enough so that ∇u is continuous), we get

$$\sum_{K \in \xi_h} \int_K \nabla u \cdot \nabla v dx - \sum_{e \in \Gamma_0 \cup \Gamma^D} \int_e \{\nabla u\} \cdot [v] ds = \sum_{K \in \xi_h} \int_K f v dx + \sum_{e \in \Gamma_N} \int_e g^N v ds$$

Yet, the left hand side is not coercive, even not symmetric. To handle this, noting that $[u] = 0$ along the interior edges (u is assumed to be continuous), we reach at

$$\begin{aligned} & \sum_{K \in \xi_h} \int_K \nabla u \cdot \nabla v dx - \sum_{e \in \Gamma_0 \cup \Gamma^D} \int_e \{\nabla u\} \cdot [v] ds - \sum_{e \in \Gamma_0} \int_e \{\nabla v\} \cdot [u] ds \\ & + \sum_{e \in \Gamma_0} \frac{\sigma}{h_e} \int_e [u] \cdot [v] ds = \sum_{K \in \xi_h} \int_K f v dx + \sum_{e \in \Gamma_N} \int_e g^N v ds \end{aligned}$$

where h_e denote the length of the edge e and σ is called the penalty parameter, which is a sufficiently large to have the coercivity. Finally, we add to the both sides the edge integrals on the Dirichlet boundary edges (keeping unknown on the left hand side and imposing Dirichlet boundary condition on the right hand side)

$$\begin{aligned} & \sum_{K \in \xi_h} \int_K \nabla u \cdot \nabla v dx - \sum_{e \in \Gamma_0 \cup \Gamma^D} \int_e \{\nabla u\} \cdot [v] ds - \sum_{e \in \Gamma_0 \cup \Gamma^D} \int_e \{\nabla v\} \cdot [u] ds \\ & + \sum_{e \in \Gamma_0 \cup \Gamma^D} \frac{\sigma}{h_e} \int_e [u] \cdot [v] ds = \sum_{K \in \xi_h} \int_K f v dx + \sum_{e \in \Gamma_D} \int_e g^D \left(\frac{\sigma}{h_e} v - \nabla v \cdot \mathbf{n} \right) ds + \sum_{e \in \Gamma_N} \int_e g^N v ds \end{aligned}$$

which gives the SIPG formulation.

Now, we give the SIPG discretized system to the problem (1) combining with the upwind discretization for the convection part: find $u_h \in V_h$ such that

$$a_h(u_h, v_h) + b_h(u_h, v_h) = l_h(v_h) \quad \forall v_h \in V_h, \quad (5)$$

$$\begin{aligned}
a_h(u_h, v_h) &= \sum_{K \in \xi_h} \int_K \epsilon \nabla u_h \cdot \nabla v_h dx + \sum_{K \in \xi_h} \int_K (\mathbf{b} \cdot \nabla u_h + \alpha u_h) v_h dx \\
&\quad - \sum_{e \in \Gamma_0 \cup \Gamma^D} \int_e \{\epsilon \nabla v_h\} \cdot [u_h] ds - \sum_{e \in \Gamma_0 \cup \Gamma^D} \int_e \{\epsilon \nabla u_h\} \cdot [v_h] ds \\
&\quad + \sum_{K \in \xi_h} \int_{\partial K^- \setminus \partial \Omega} \mathbf{b} \cdot \mathbf{n} (u_h^{out} - u_h^{in}) v_h ds - \sum_{K \in \xi_h} \int_{\partial K^- \cap \Gamma^-} \mathbf{b} \cdot \mathbf{n} u_h^{in} v_h ds \\
&\quad + \sum_{e \in \Gamma_0 \cup \Gamma^D} \frac{\sigma \epsilon}{h_e} \int_e [u_h] \cdot [v_h] ds, \\
b_h(u_h, v_h) &= \sum_{K \in \xi_h} \int_K r(u_h) v_h dx, \\
l_h(v_h) &= \sum_{K \in \xi_h} \int_K f v_h dx + \sum_{e \in \Gamma^D} \int_e g^D \left(\frac{\sigma \epsilon}{h_e} v_h - \epsilon \nabla v_h \cdot \mathbf{n} \right) ds \\
&\quad - \sum_{K \in \xi_h} \int_{\partial K^- \cap \Gamma^-} \mathbf{b} \cdot \mathbf{n} g^D v_h ds + \sum_{e \in \Gamma^N} \int_e g^N v_h ds,
\end{aligned}$$

where ∂K^- and Γ^- indicates the corresponding inflow parts, and u_h^{out} , u_h^{in} denotes the values on an edge from outside and inside of an element K , respectively. The parameter $\sigma \in \mathbb{R}_0^+$ is called the penalty parameter which should be sufficiently large; independent of the mesh size h and the diffusion coefficient ϵ (Rivière, 2008) [Sec. 2.7.1]. We choose the penalty parameter σ for the SIPG method depending on the polynomial degree k as $\sigma = 3k(k+1)$ on interior edges and $\sigma = 6k(k+1)$ on boundary edges.

3. Adaptivity

Most of the convection dominated problems lead to internal/boundary layers and one has to find accurate approximations in order to handle the nonphysical oscillations. A naive approach is to refine the mesh uniformly. But it is not desirable as it highly increases the degrees of freedom and refines the mesh unnecessarily in regions where the solutions are smooth. Instead, the mesh is refined locally using an adaptive strategy. In this section, we describe the adaptive strategy for non-linear diffusion-convection-reaction problems.

3.1. The adaptive procedure

Our adaptive algorithm is based on the standard adaptive finite element (AFEM) iterative loop (Fig.2). The first step, SOLVE, is to solve the SIPG discretized system (5) on a given triangulation ξ_h . The ESTIMATE step is the key part of the adaptive procedure, by which we are able to determine the elements having large error to be refined using computed solution and given data (a posteriori). As an estimator, we use a residual based error indicator based on the modification of the error estimator given in Schötzau and Zhu (Schötzau & Zhu, 2009) for a single linear convection dominated diffusion-convection-reaction equation to the diffusion-convection equation with non-linear reaction mechanism, which is robust, i.e. independent of the Péclet number. To do this, we include in the a posteriori error indicator the non-linear reaction

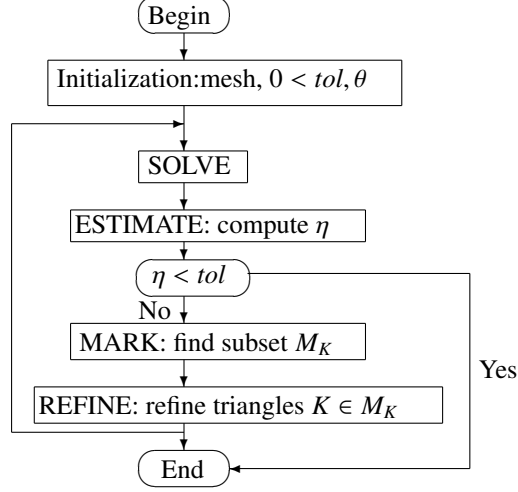


Figure 2: Adaptive strategy

term as local contributions to the cell residuals and not to the interior/boundary edge residuals [Chp. 5.1.4, (Verfürth, 2013)]. Let u_h be the solution to (5). Then, for each element $K \in \xi_h$, we define the local error indicators η_K^2 as

$$\eta_K^2 = \eta_{R_K}^2 + \eta_{E_K^0}^2 + \eta_{E_K^D}^2 + \eta_{E_K^N}^2, \quad (7)$$

In (7), η_{R_K} denote the cell residual

$$\eta_{R_K}^2 = \rho_K^2 \|f - \alpha u_h + \epsilon \Delta u_h - \mathbf{b} \cdot \nabla u_h - r(u_h)\|_{L^2(K)}^2,$$

while, $\eta_{E_K^0}$, $\eta_{E_K^D}$ and $\eta_{E_K^N}$ stand for the edge residuals coming from the jump of the numerical solution on the interior, Dirichlet boundary and Neumann boundary edges, respectively

$$\begin{aligned} \eta_{E_K^0}^2 &= \sum_{e \in \partial K \cap \Gamma_0} \left(\frac{1}{2} \epsilon^{-\frac{1}{2}} \rho_e \|[\epsilon \nabla u_h]\|_{L^2(e)}^2 + \frac{1}{2} \left(\frac{\epsilon \sigma}{h_e} + \kappa h_e + \frac{h_e}{\epsilon} \right) \| [u_h] \|_{L^2(e)}^2 \right), \\ \eta_{E_K^D}^2 &= \sum_{e \in \partial K \cap \Gamma^D} \left(\frac{\epsilon \sigma}{h_e} + \kappa h_e + \frac{h_e}{\epsilon} \right) \|g^D - u_h\|_{L^2(e)}^2, \\ \eta_{E_K^N}^2 &= \sum_{e \in \partial K \cap \Gamma^N} \epsilon^{-\frac{1}{2}} \rho_e \|g^N - \epsilon \nabla u_h \cdot \mathbf{n}\|_{L^2(e)}^2, \end{aligned}$$

as in Schötzau and Zhu (Schötzau & Zhu, 2009) with the modified (Hoppe et al., 2008; Schötzau & Zhu, 2009) extra term $\eta_{E_K^N}^2$ corresponding to the local indicator on the Neumann boundary edges. The weights ρ_K and ρ_e , on an element K , are defined as

$$\rho_K = \min\{h_K \epsilon^{-\frac{1}{2}}, \kappa^{-\frac{1}{2}}\}, \quad \rho_e = \min\{h_e \epsilon^{-\frac{1}{2}}, \kappa^{-\frac{1}{2}}\},$$

for $\kappa \neq 0$. When $\kappa = 0$, we take $\rho_K = h_K \epsilon^{-\frac{1}{2}}$ and $\rho_e = h_e \epsilon^{-\frac{1}{2}}$. Then, our a posteriori error indicator is given by

$$\eta = \left(\sum_{K \in \xi_h} \eta_K^2 \right)^{1/2}.$$

We also introduce the data approximation error,

$$\Theta^2 = \Theta^2(f) + \Theta^2(u^D) + \Theta^2(u^N)$$

where

$$\begin{aligned} \Theta^2(f) &= \sum_{K \in \xi} \rho_K^2 (\|f - f_h\|_{L^2(K)}^2 + \|(\mathbf{b} - \mathbf{b}_h) \cdot \nabla u_h\|_{L^2(K)}^2 + \|(\alpha - \alpha_h) u_h\|_{L^2(K)}^2), \\ \Theta^2(u^D) &= \sum_{e \in \Gamma^D} \left(\frac{\epsilon \sigma}{h_e} + \kappa h_e + \frac{h_e}{\epsilon} \right) \|g^D - \hat{g}^D\|_{L^2(e)}^2, \\ \Theta^2(u^N) &= \sum_{e \in \Gamma^N} \epsilon^{-\frac{1}{2}} \rho_e \|g^N - \hat{g}^N\|_{L^2(e)}^2, \end{aligned}$$

according to (Schötzau & Zhu, 2009), with \hat{g}^D and \hat{g}^N denoting the mean integrals of g^D and g^N , respectively.

In the MARK step, if the given tolerance is not satisfied, we determine the set of elements $M_K \subset \xi_h$ to be refined using the error indicator defined in (7). To do this, we use the bulk criterion proposed by Döfler (Dörfler, 1996), by which the approximation error is decreased by a fixed factor for each loop. In the light of bulk criterion, we choose the set of elements $M_K \subset \xi_h$ satisfying

$$\sum_{K \in M_K} \eta_K^2 \geq \theta \sum_{K \in \xi_h} \eta_K^2,$$

for a user defined parameter $0 < \theta < 1$. Here, bigger θ results in more refinement of triangles in a single loop, where, smaller θ causes more refinement loops.

Finally, REFINED step, we refine the marked elements $K \in M_K$ using the newest vertex bisection method (Chen, 2008). This process can be summarized as (see Fig.3): for each element $K \in \xi_h$, we label one vertex of K as a newest vertex. The opposite edge of the newest vertex is called as the refinement edge. Then, a triangle is bisected to two new children triangles by connecting the newest vertex to the midpoint of the refinement edge, and this new vertex created at the midpoint of the refinement edge is assigned to be the newest vertex of the children. Following a similar rule, these two children triangles are bisected to obtain four children elements belonging to the father element (the refined triangle $K \in M_K$). After bisecting all $K \in M_K$, we also divide some elements $K \in \xi_h \setminus M_K$ to keep the conformity of the mesh, i.e. hanging nodes are not allowed.

In the case of coupled problems, instead of a single component problem, we refine the elements being the union of the set of the elements to be refined for each component, i.e., let η_K^1 and η_K^2 be the computed local error indicators corresponding to each unknown component of a two component system. Next, we determine the set of elements M_K^1 and M_K^2 satisfying

$$\sum_{K \in M_K^1} (\eta_K^1)^2 \geq \theta \sum_{K \in \xi_h} (\eta_K^1)^2, \quad \sum_{K \in M_K^2} (\eta_K^2)^2 \geq \theta \sum_{K \in \xi_h} (\eta_K^2)^2.$$

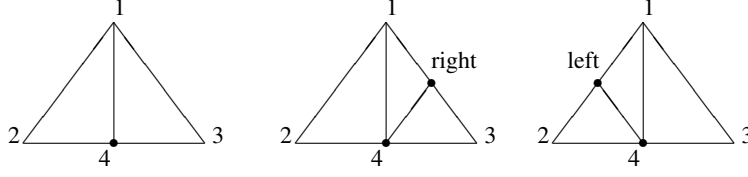


Figure 3: Bisection of a triangle

Then, we refine the marked elements $K \in M_K^1 \cup M_K^2$ using the newest vertex bisection method. The adaptive procedure ends after a sequence of mesh refinements up to attain a solution with an estimated error within a prescribed tolerance. Numerical studies show the capability of the error indicator to find the layers properly.

3.2. Reliability and efficiency of a posteriori error estimator

In order to measure the error, we use the energy norm

$$|||v|||^2 = \sum_{K \in \xi_h} (\|\epsilon \nabla v\|_{L^2(K)}^2 + \kappa \|v\|_{L^2(K)}^2) + \sum_{e \in \Gamma_0 \cup \Gamma^D} \frac{\epsilon \sigma}{h_e} \|[v]\|_{L^2(e)}^2,$$

and the semi-norm

$$|v|_C^2 = |\mathbf{b}v|_*^2 + \sum_{e \in \Gamma_0 \cup \Gamma^D} (\kappa h_e + \frac{h_e}{\epsilon}) \|[v]\|_{L^2(e)}^2, \quad (8)$$

where

$$|u|_* = \sup_{w \in H_0^1(\Omega) \setminus \{0\}} \frac{\int_{\Omega} u \cdot \nabla w dx}{|||w|||},$$

and the constant $\kappa \geq 0$ satisfies

$$\alpha - \frac{1}{2} \nabla \cdot \mathbf{b}(x) \geq \kappa, \quad \| - \nabla \cdot \mathbf{b} + \alpha \|_{L^\infty(\Omega)} \leq \kappa^* \kappa, \quad (9)$$

for a non-negative κ^* . The first condition in (9) is needed to make the bilinear form a_h coercive (well-posedness of the linear part of the problem), and the latter is used to prove the reliability of our a posteriori error estimator (Schötzau & Zhu, 2009). The terms $|\mathbf{b}v|_*^2$ and $\frac{h_e}{\epsilon} \|[v]\|_{L^2(e)}^2$ in (8) are used to bound the convection part, whereas, the term $\kappa h_e \|[v]\|_{L^2(e)}^2$ is used to bound the linear reaction part of the discrete system. In order to bound the non-linear reaction part, we use the boundedness property (2a) [Chp. 5.1.1-4, (Verfürth, 2013)]. Then, for the solution u to the scalar equation of (1), following the procedures in (Schötzau & Zhu, 2009) and using the boundedness of the non-linear reaction term, we can easily obtain the a posteriori error bounds

$$|||u - u_h||| + |u - u_h|_C \lesssim \eta + \Theta \quad (\text{reliability}),$$

$$\eta \lesssim |||u - u_h||| + |u - u_h|_C + \Theta \quad (\text{efficiency}).$$

4. Comparison with the Galerkin least squares finite element method (GLSFEM)

For linear PDEs, the weak form in the standard Galerkin method is obtained by multiplying the differential equation with a test function v and integrating over a suitable function space V

$$(\mathcal{L}u, v) = (f, v), \quad \forall v \in V$$

where $\mathcal{L} = -\epsilon\Delta + \mathbf{b} \cdot \nabla + \alpha$ is the linear part of the diffusion-convection-reaction equation (1). Defining the residual as $R(u) = f - \mathcal{L}u$, the standard Galerkin method can be interpreted in form of the residual orthogonality $(R(u), v) = 0$. In the case of non self-adjoint differential operators like the diffusion-convection-reaction operator \mathcal{L} , it can happen that $(\mathcal{L}u, v)$ is not coercive or symmetric on V , and the resulting FEM discretization may be unstable.

For transport problems, another popular approach is based on the least squares formulation of the Galerkin FEM. Let us write the model problem (1) as

$$\mathcal{L}u + r(u) = f \quad \text{in } \Omega \tag{10a}$$

$$u = g \quad \text{on } \Gamma, \tag{10b}$$

Define the least-squares functional

$$J(u) := \frac{1}{2} \|\mathcal{L}u + r(u) - f\|_{L^2(\Omega)}^2.$$

A minimizer of $J(u)$ is obtained by

$$\lim_{t \rightarrow 0} \frac{d}{dt} J(u + tv) = 0, \quad \forall v \in V$$

which yields the least-squares term

$$\tilde{J}_\Omega(u, v) := (\mathcal{L}u + r(u) - f, \mathcal{L}v + r'(u)v)_{L^2(\Omega)}.$$

For linear problems with $r(u) = 0$, the least squares Galerkin method reduces to the minimization problem

$$F(u) = \min_{v \in V} F(v)$$

where the functional $F(\cdot)$ is defined by

$$F(v) = \frac{1}{2} \|\mathcal{L}v - f\|_{L^2(\Omega)}^2.$$

The first order optimality condition leads to the least squares Galerkin method

$$(\mathcal{L}u, \mathcal{L}v) = (f, \mathcal{L}v), \quad \forall v \in V.$$

The bilinear form $(\mathcal{L}u, \mathcal{L}v)$ is symmetric and coercive and has stronger stability properties compared to the standard Galerkin method.

There are many publications on the Galerkin least squares finite element methods (GLSFEM). We mention here two books (Bochev & Gunzburger, 2009; Jiang, 1998) and the review article (Bochev & Gunzburger, 1998). There are mainly two variants of the GLSFEMs; the stabilized and the direct versions.

Stabilized finite elements method (Hughes, et al., 1989): The standard (continuous) Galerkin FEM for the problem (10) reads: find $u_h \in U_h \subset U$ such that

$$a(u_h, v_h) + (r(u_h), v_h)_{L^2(\Omega)} = (f, v_h)_{L^2(\Omega)}, \quad \forall v_h \in V_h \subset V \quad (11)$$

where $a(u, v) = (\epsilon \nabla u + \mathbf{b} \cdot \nabla u + \alpha u, v)_{L^2(\Omega)}$ is the standard bilinear form to the linear part of (10). The general stabilized FEMs formulation reads as: for all $v_h \in V_h \subset V$, find $u_h \in U_h \subset U$ such that

$$a(u_h, v_h) + (r(u_h), v_h)_{L^2(\Omega)} + \sum_K \tau_K \mathbf{S}_K(\mathbf{u}_h, \mathbf{v}_h) = (f, v_h)_{L^2(\Omega)} \quad (12)$$

where the stabilization parameter is defined on each element K as (Hauke, 2002)

$$\tau_K = \frac{1}{\frac{4\epsilon}{h^2} + \frac{2|\mathbf{b}|}{h} + |\alpha|}.$$

One way to proceed GLSFEMs is then to use the least-squares term $\tilde{J}_K(u, v)$ as the stabilization term S_K in (12), i.e.: for all $v_h \in V_h$, find $u_h \in U_h$ such that

$$a(u_h, v_h) + (r(u_h), v_h)_{L^2(\Omega)} + \sum_K \tau_K \tilde{J}_K(u_h, v_h) = (f, v_h)_{L^2(\Omega)} \quad (13)$$

Note that, being another stabilized FEM, streamline upwind Petrov-Galerkin (SUPG) method is obtained by setting

$$S_K(u_h, v_h) = (\mathcal{L}u_h + r(u_h) - f, \mathbf{b} \cdot \nabla v_h)_{L^2(K)}$$

with different choices of the parameter τ_K .

The direct variant of GLSFEM: The second way to proceed the GLSFEMs is to consider and discretize just the least-squares term $\tilde{J}_\Omega(u, v)$. One may solve this problem in a straightforward manner: for all $v_h \in V_h \subset H^2(\Omega) \cap V$, find $u_h \in U_h \subset H^2(\Omega) \cap U$ such that $\tilde{J}_\Omega(u_h, v_h) = 0$, i.e.

$$\int_\Omega (\mathcal{L}u_h + r(u_h))(\mathcal{L}v_h + r'(u_h)v_h)dx = \int_\Omega f(\mathcal{L}v_h + r'(u_h)v_h)dx$$

which is not only a fourth order problem but also the solution and trial subspaces U_h and V_h need to consist of continuously differentiable functions making it complicated to construct bases functions (standard finite element spaces cannot be used anymore) and the assembly of the stiffness matrix. The condition number of the stiffness matrix is order of $\mathcal{O}(h^{-4})$ instead of order $\mathcal{O}(h^{-2})$ for the standard Galerkin FEM. Hence, this approach is impractical. Instead, being the most common practical way, the problem (10) is converted into a first-order system as (Houston et al., 2002; Bochev & Gunzburger, 1998).

$$\begin{aligned} p - \nabla u &= 0 & \text{in } \Omega \\ -\epsilon \nabla \cdot p + \mathbf{b} \cdot \nabla u + \alpha u + r(u) &= f & \text{in } \Omega \\ u &= g & \text{on } \Gamma \end{aligned}$$

Then, we define now the least-square functional for $z = (p, u)^T$ as

$$J(z) := \frac{1}{2} \|p - \nabla u\|_{L^2(\Omega)}^2 + \frac{1}{2} \|-\epsilon \nabla \cdot p + \mathbf{b} \cdot \nabla u + \alpha u + r(u) - f\|_{L^2(\Omega)}^2$$

A minimizer of $J(z)$ is obtained by the identity

$$\lim_{t \rightarrow 0} \frac{d}{dt} J(z + tv) = 0, \quad \forall v$$

which yields a least-squares term of order two. Using this approach, we solve the resulting least-squares term, which is a second-order problem now, using (discontinuous) finite elements solution and trial spaces $S_h \subset H^1(\Omega, \text{div}) \times U$ ($S_h \subset H^1(\Omega, \text{div}) \times H^1(\Omega)$) and $T_h \subset H^1(\Omega, \text{div}) \times V$ ($T_h \subset H^1(\Omega, \text{div}) \times H^1(\Omega)$), respectively. The condition number of the stiffness matrix is retained as $O(h^{-2})$ as in the standard Galerkin method (Bochev & Gunzburger, 1998). For convection dominated problems, the resulting linear systems of equations are solved usually with preconditioned conjugate gradient method due to large condition numbers, as reported in (Lazarov & Vassilevski, 2000) for GLSFEM solution of singularly perturbed diffusion-convection problems.

In order to compare the GLSFEM with the DGFEM, we consider the linear problem (Yücel et al., 2013)

$$-\epsilon \Delta u + \mathbf{b} \cdot \nabla u + \alpha u = f \quad \text{in } (0, 1)^2 \quad (14)$$

with $\epsilon = 10^{-6}$, $\beta = (2, 3)^T$ and $\alpha = 1$. The load function f and Dirichlet boundary conditions are chosen so that the exact solution is

$$u(x_1, x_2) = \frac{\pi}{2} \arctan\left(\frac{1}{\sqrt{\epsilon}}(-0.5x_1 + x_2 - 0.25)\right)$$

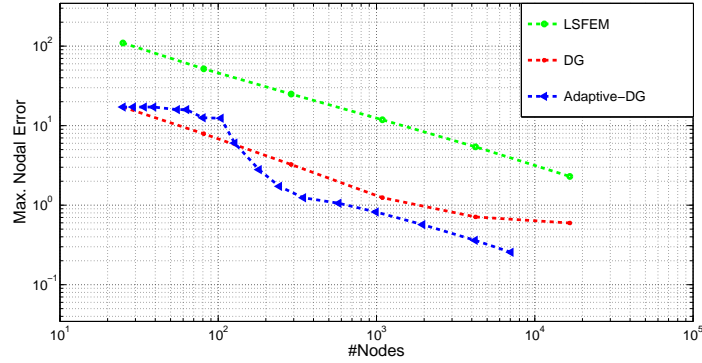


Figure 4: Comparison of the GLSFEM and DGFEM for linear convection dominated problem (14)

As we can see from the from the Fig.4, the DGFEMs produce smaller errors than the GLSFEM for the convection dominated problem (14).

5. Efficient solution of linear systems

The approximate solution to the discrete problem (5) has the form

$$u_h = \sum_{i=1}^{Nel} \sum_{l=1}^{Nloc} U_l^i \phi_l^i$$

where ϕ_l^i 's are the basis polynomials spanning the DGFEM space V_h , U_l^i 's are the unknown coefficients to be found, Nel denotes the number of triangles and $Nloc$ is the number of local dimension depending on the degree of polynomials k , for instance, for $k = 2$ we have $Nloc = 6$ (in 2D, $Nloc = (k + 1)(k + 2)/2$). In DG methods, we choose the piecewise basis polynomials ϕ_l^i 's in such a way that each basis function has only one triangle as a support, i.e. we choose on a specific triangle K_e , $e \in \{1, 2, \dots, Nel\}$, the basis polynomials ϕ_l^e which are zero outside the triangle K_e , $l = 1, 2, \dots, Nloc$. By this construction, the stiffness matrix obtained by DG methods has a block structure, each of which related to a triangle (there is no overlapping as in continuous FEM case). The product $dof := Nel * Nloc$ gives the degree of freedom in DG methods. Inserting the linear combination of u_h in (5) and choosing the test functions as $v_h = \phi_l^i$, $l = 1, 2, \dots, Nloc$, $i = 1, 2, \dots, Nel$, the discrete residual of the system (5) in matrix vector form is given by

$$R(\mathbf{U}) = S\mathbf{U} + h(\mathbf{U}) - L$$

where $\mathbf{U} \in \mathbb{R}^{dof}$ is the vector of unknown coefficients U_l^i 's, $S \in \mathbb{R}^{dof \times dof}$ is the stiffness matrix corresponding to the bilinear form $a_h(u_h, v_h)$, $h \in \mathbb{R}^{dof}$ is the vector function of U related to the non-linear form $b_h(u_h, v_h)$ and $L \in \mathbb{R}^{dof}$ is the vector to the linear form $l_h(v_h)$. The explicit definitions are given by

$$S = \begin{bmatrix} S_{11} & S_{12} & \cdots & S_{1,Nel} \\ S_{21} & S_{22} & & \vdots \\ \vdots & & \ddots & \\ S_{Nel,1} & \cdots & & S_{Nel,Nel} \end{bmatrix}, \quad \mathbf{U} = \begin{bmatrix} \mathbf{U}_1 \\ \mathbf{U}_2 \\ \vdots \\ \mathbf{U}_{Nel} \end{bmatrix}$$

$$h(\mathbf{U}) = \begin{bmatrix} \mathbf{h}_1 \\ \mathbf{h}_2 \\ \vdots \\ \mathbf{h}_{Nel} \end{bmatrix}, \quad L = \begin{bmatrix} \mathbf{L}_1 \\ \mathbf{L}_2 \\ \vdots \\ \mathbf{L}_{Nel} \end{bmatrix}$$

where all the block matrices have dimension $Nloc$:

$$S_{ji} = \begin{bmatrix} a_h(\phi_1^i, \phi_1^j) & a_h(\phi_2^i, \phi_1^j) & \cdots & a_h(\phi_{Nloc}^i, \phi_1^j) \\ a_h(\phi_1^i, \phi_2^j) & a_h(\phi_2^i, \phi_2^j) & & \vdots \\ \vdots & & \ddots & \\ a_h(\phi_1^i, \phi_{Nloc}^j) & \cdots & & a_h(\phi_{Nloc}^i, \phi_{Nloc}^j) \end{bmatrix}, \quad \mathbf{U}_i = \begin{bmatrix} U_1^i \\ U_2^i \\ \vdots \\ U_{Nloc}^i \end{bmatrix}$$

$$\mathbf{h}_i = \begin{bmatrix} b_h(u_h, \phi_1^i) \\ b_h(u_h, \phi_2^i) \\ \vdots \\ b_h(u_h, \phi_{Nloc}^i) \end{bmatrix}, \quad \mathbf{L}_i = \begin{bmatrix} l_h(\phi_1^i) \\ l_h(\phi_2^i) \\ \vdots \\ l_h(\phi_{Nloc}^i) \end{bmatrix}$$

Obviously, the condition number of the stiffness matrix obtained by the SIPG discretization increases by the degree k of basis polynomials. One of the reasonable ways to handle this drawback is to choose a suitable set of basis polynomials. There are a variety of basis polynomial

functions such as Lagrange shape functions, monomial bases, Legendre polynomials. In our study, we use the orthogonal Dubiner basis defined on the reference triangle (Deng & Cai, 2005)

$$\hat{T} = \{\mathbf{x} = (x_1, x_2) | 0 \leq x_1, x_2 \leq 1\}$$

(all the integral terms above are computed on this reference triangle using an affine map between the reference triangle and physical triangles). The construction of such basis polynomials based on the collapsed coordinate transform between the reference triangle \hat{T} and the reference square $\hat{Q} = [-1, 1]^2$ (see Fig.5). First, the basis polynomials on the square \hat{Q} is formed by a generalized

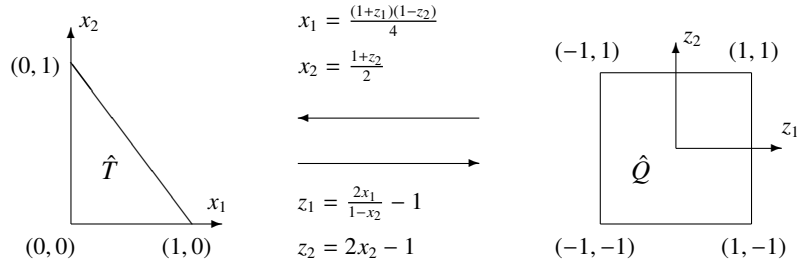


Figure 5: Collapsed coordinate transform between reference triangle and reference square

tensor product of the Jacobi polynomials on the interval $[-1, 1]$, and then, these basis polynomials are transformed to the reference triangle \hat{T} using the collapsed coordinate transform in Fig.5. The explicit forms of Dubiner basis polynomials on the reference triangle \hat{T} are given by

$$\begin{aligned} \phi_{mn}(x_1, x_2) &= (1 - z_2)^m P_m^{0,0}(z_1) P_n^{2m+1,0}(z_2) \\ &= 2^m (1 - x_2)^m P_m^{0,0}\left(\frac{2x_1}{1-x_2} - 1\right) P_n^{2m+1,0}(2x_2 - 1), \quad 0 \leq m, n, m+n \leq N_{loc} \end{aligned}$$

where $P_n^{\alpha,\beta}(x)$'s denote the corresponding n -th order Jacobi polynomials on the interval $[-1, 1]$, which are orthogonal polynomials under the Jacobi weight $(1-x)^\alpha(1+x)^\beta$, i.e.

$$\int_{-1}^1 (1-x)^\alpha (1+x)^\beta P_m^{\alpha,\beta}(x) P_n^{\alpha,\beta}(x) dx = \delta_{mn}$$

This property of the Jacobi polynomials yields the orthogonality of the Dubiner basis on the reference triangle \hat{T} as

$$\iint_{\hat{T}} \phi_{mn}(x_1, x_2) \phi_{ij}(x_1, x_2) dx_1 dx_2 = \frac{1}{8} \delta_{mi} \delta_{nj}.$$

The advantage of the Dubiner basis is that its orthogonality leads to diagonal mass matrix by which one may obtain better-conditioned matrices compared to the other basis polynomials (see Fig.6), and it provides high accuracy in the approximation of the integrals.

5.1. Effect of the penalty parameter

The penalty parameter σ in the SIPG formulation (5) should be selected sufficiently large to ensure the coercivity of the bilinear form [(Rivière, 2008), Sec. 27.1], which is needed for

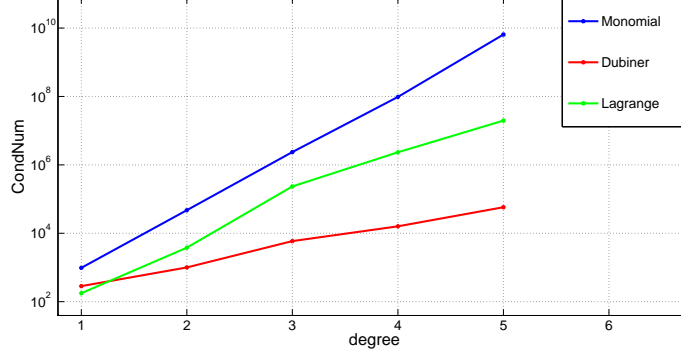


Figure 6: Degree vs. condition number of the stiffness matrix: comparison for different type of basis functions for the linear model problem (1) with $r(u) = 0$

the stability of the convergence of the DG method. It ensures that the matrix arising from the DG discretization of the diffusion part of (5) is symmetric positive definite. At the same time it should not be too large since the conditioning of the matrix arising from the bilinear form increases linearly by the penalty parameter (see Fig.7). In the literature, several choices of the penalty parameter are suggested. In (Epshteyn & Rivi re, 2007), computable lower bounds are derived, and in (Dobrev et al., 2008), the penalty parameter is chosen depending on the diffusion coefficient ϵ . The effect of the penalty parameter on the condition number was discussed in detail for the DG discretization of the Poisson equation in (Castillo, 2012) and in (Slingerland & Vuik, 2014) for layered reservoirs with strong permeability contrasts, e.g. ϵ varying between 10^{-1} and 10^{-7} . Since the penalty parameter, in SIPG formulation, is mainly related to the Laplace operator, to examine the effect of the penalty parameter, we study on the Poisson problem (pure elliptic case)

$$-\Delta u = f \quad \text{in } (0, 1)^2 \quad (15)$$

with the appropriate load function f and Dirichlet boundary conditions using the exact solution $u(x) = \sin(\pi x_1) \sin(\pi x_2)$. In Fig.8, we have plotted the maximum nodal errors for the Poisson problem (15) depending on the penalty parameter to show the instability bound of the scheme for different degrees of bases, where the triangular symbols indicate our choice $\sigma = 3k(k + 1)$.

Similarly, the condition number of the stiffness matrix increases with decreasing mesh-size and increasing order of the DG discretization for the linear diffusion-convection-reaction problem (3) with $r(u) = 0$, (see Fig.9), which affects the efficiency of an iterative solver. Similar results can be found in (Castillo, 2012) for the Poisson problem.

Besides the choice of a suitable basis polynomials, in this section, we describe also an efficient solution technique for the large ill-conditioned linear systems arising from the linearization of the DG discretization. This technique is based on reordering of matrix elements and preconditioning.

5.2. Matrix reordering & block LU factorization

Because the stiffness matrices obtained by DGFEM become ill-conditioned and dense for higher order DG elements (Ayuso & Marini, 2009), several preconditioners are developed for

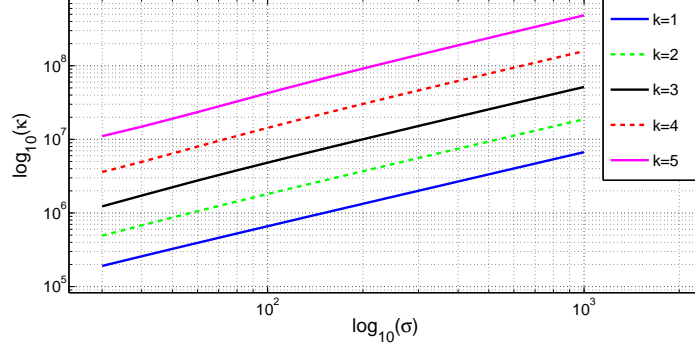


Figure 7: Condition number of the stiffness matrix of the SIPG method as a function of penalty parameter σ with different polynomial degree k for the Poisson equation (15)

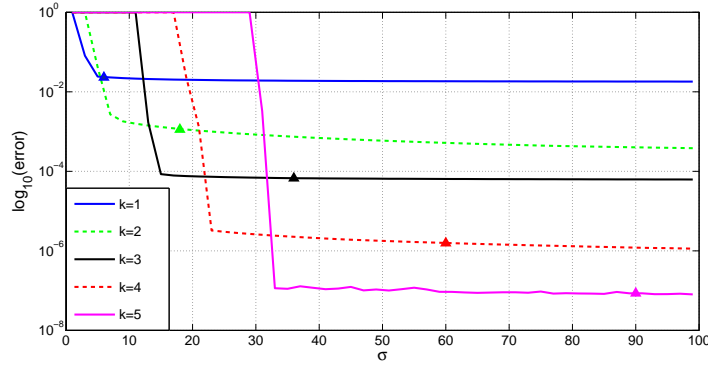


Figure 8: Maximum nodal errors of the SIPG approximation as a function of penalty parameter σ with different polynomial degree k for the Poisson equation (15)

the efficient and accurate solution of linear diffusion-convection equations (Antonietti & Süli, 2009; Georgoulis & Loghin, 2008). We apply the matrix reordering and partitioning technique in (Tari & Manguoğlu, 2013), which uses the largest eigenvalue and corresponding eigenvector of the Laplacian matrix. This reordering allows us to obtain a partitioning and a preconditioner based on this partitioning. Since our matrices are non-symmetric, as the first step, we compute the symmetric structure by adding its transpose to itself. A symmetric, square and sparse matrix could be represented as a graph where same index rows and columns are mapped into vertices and nonzeros of the sparse matrix are mapped into the edges of the graph. Since the matrix is symmetric, the corresponding graph is undirected. The Laplacian matrix (\mathcal{L}) is, then, defined as follows

$$\mathcal{L}(i, j) = \begin{cases} \deg(v_i) & \text{if } i = j, \\ -1 & \text{if } i \neq j \end{cases}$$

in which the $\deg(v_i)$ is the degree of the vertex i . In this paper, the reordering we use is based on the unweighted Laplacian matrix given above. If the graph contains only one connected

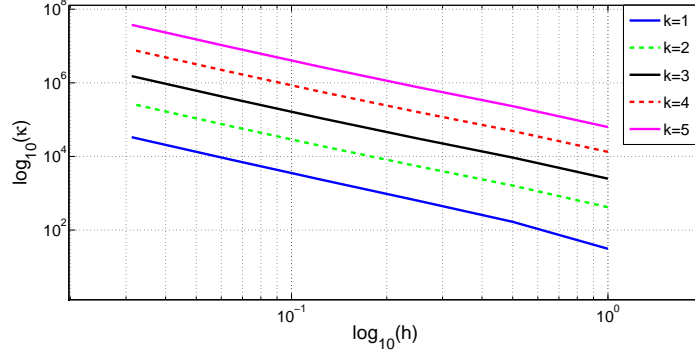


Figure 9: Condition number of the stiffness matrix of the SIPG method as a function of mesh-size h with different polynomial degree k for the linear model problem (1) with $r(u) = 0$

component, the eigenvalues of \mathcal{L} are $0 = \lambda_1 < \lambda_2 \leq \lambda_3 \leq \dots \leq \lambda_n$, otherwise there are as many zero eigenvalues as the number of connected components.

Certain eigenvalues and corresponding eigenvectors of the Laplacian matrix have been studied extensively. Most notably the second nontrivial eigenvalue of the Laplacian and the corresponding eigenvector known as the algebraic connectivity and the Fiedler vector of the graph (Fiedler, 1973). Nodal domain theorem in (Fiedler, 1975) shows that the eigenvectors corresponding to the eigenvalues other than the first and the second smallest eigenvalue give us the connected components of the graph. In (Barnard et al., 1995), the Fiedler vector for permuting the matrices to reduce the bandwidth is proposed. Reordering to obtain effective and scalable parallel banded preconditioners is proposed in (Manguoğlu et al., 2010). We use a sparse matrix reordering for partitioning and solving linear systems using the largest eigenvalue and the corresponding eigenvector of the Laplacian matrix. Using this reordering, we show that one can reveal underlying structure of a sparse matrix. A simple Matlab code to find the reordered matrix and the permutation matrix can be found at (<http://www.ceng.metu.edu.tr/~manguoglu/MatrixReorder.m>)

To solve the discrete problem (5), we use the Newton-Raphson method. We start with a non-zero initial vector $\mathbf{U}^{(0)}$. The linear system arising from i^{th} -Newton-Raphson iteration step has the form $J\mathbf{w}^{(i)} = -\mathbf{R}^{(i)}$, where J is the Jacobian matrix to $\mathbf{R}(\mathbf{U}^{(0)})$ (i.e. $J = S + h'(\mathbf{U}^{(0)})$) and it remains unchanged among the iteration steps), $\mathbf{w}^{(i)} = \mathbf{U}^{(i+1)} - \mathbf{U}^{(i)}$ is the Newton correction, and $\mathbf{R}^{(i)}$ denotes the residual of the system at $\mathbf{U}^{(i)}$ ($\mathbf{R}^{(i)} = \mathbf{R}(\mathbf{U}^{(i)})$). We construct a permutation matrix P using the matrix reordering technique described above, applied to the sparse matrix J . Then, we apply the permutation matrix P to obtain the permuted system $N\mathbf{w} = \mathbf{d}$ where $N = PJP^T$, $\mathbf{w} = P\mathbf{w}^{(i)}$ and $\mathbf{d} = -P\mathbf{R}^{(i)}$. After solving the permuted system, the solution of the unpermuted linear system can be obtained by applying the inverse permutation, $\mathbf{w}^{(i)} = P^T\mathbf{w}$. Given a sparse linear system of equations $N\mathbf{w} = \mathbf{d}$, after reordering, one way to solve this system is via block LU factorization. Suppose, the permuted matrix N , the right hand side \mathbf{d} and the solution \mathbf{w} is partitioned as follows:

$$\begin{pmatrix} A & B \\ C^T & D \end{pmatrix} \begin{pmatrix} \mathbf{w}_1 \\ \mathbf{w}_2 \end{pmatrix} = \begin{pmatrix} \mathbf{d}_1 \\ \mathbf{d}_2 \end{pmatrix}$$

A block LU factorization of the coefficient matrix can be given as

$$\begin{pmatrix} A & B \\ C^T & D \end{pmatrix} = \begin{pmatrix} A & 0 \\ C^T & S \end{pmatrix} \begin{pmatrix} I & U \\ 0 & I \end{pmatrix}$$

where $U = A^{-1}B$ and $S = D - C^T A^{-1}B$, also known as the Schur complement matrix. If the cost can be amortized, one can form U and S once and use them for solving linear systems with the same coefficient matrix and different right hand sides. After this factorization, there are various approaches that one can take to solve the system. One way is to solve the system via block backward and forward substitution, by first solving the linear system $At = d_1$, and then solving the Schur complement system $Sw_2 = d_2 - C^T t$ and obtaining $w_1 = t - Uw_2$. This method is summarized in Algorithm 1.

Algorithm 1 Algorithm for solving the linear system after reordering

Input: The coefficient matrix: $\begin{pmatrix} A & B \\ C^T & D \end{pmatrix}$ and the right hand side: $\begin{pmatrix} d_1 \\ d_2 \end{pmatrix}$
Output: The solution vector: $\begin{pmatrix} w_1 \\ w_2 \end{pmatrix}$

- 1: solve $At = d_1$
 - 2: solve $Sw_2 = d_2 - C^T t$
 - 3: compute $w_1 = t - Uw_2$
-

We note that this approach involves solving two linear systems of equations with the coefficient matrix A and S . These linear systems can be solved directly or iteratively which requires effective preconditioners. Other approaches could involve solving the system $Nw = d$ iteratively where the preconditioner could take many forms. There are many other techniques for solving block partitioned and saddle point linear systems, we refer the reader to (Benzi et al., 2005) for a more detailed survey of some of these methods.

6. Numerical results

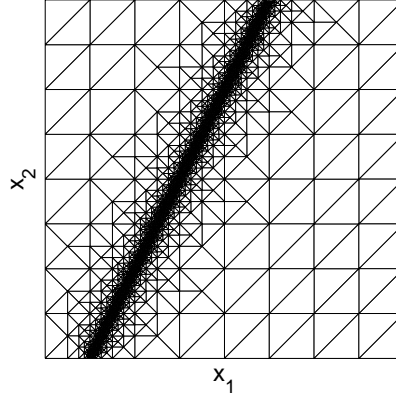
In this section, we give several numerical examples demonstrating the effectiveness and accuracy of the DGAFEM for convection dominated non-linear diffusion-convection-reaction equations.

6.1. Example with polynomial type non-linearity

Our first example is taken from (Bause, 2010) with Dirichlet boundary condition on $\Omega = (0, 1)^2$ with $\epsilon = 10^{-6}$, $\mathbf{b} = \frac{1}{\sqrt{5}}(1, 2)^T$, $\alpha = 1$ and $r(u) = u^2$. The source function f and Dirichlet boundary condition are chosen so that $u(x_1, x_2) = \frac{1}{2} \left(1 - \tanh \frac{2x_1 - x_2 - 0.25}{\sqrt{5}\epsilon} \right)$ is the exact solution. The problem is characterized by an internal layer of thickness $O(\sqrt{\epsilon} |\ln \epsilon|)$ around $2x_1 - x_2 = \frac{1}{4}$.

The mesh is locally refined by DGAFEM around the interior layer (Fig.10) and the spurious solutions are damped out in Fig.11, similar to the results as in (Bause, 2010) using SUPG-SC, in (Yücel et al., 2013) with SIPG-SC. On adaptively and uniformly refined meshes, from the Fig.12, it can be clearly seen that the adaptive meshes reduce the substantial computing time.

On uniform meshes, the SIPG is slightly more accurate as shown in (Yücel et al., 2013) than the SUPG-SC in (Bause, 2010). The error reduction by increasing degree of the polynomials is remarkable on finer adaptive meshes (Fig.12, bottom).



(a) d.o.f. 70716

Figure 10: Example 6.1: Adaptive mesh.

In Table 1, we give the results using the solution technique in Section 5 for the *BiCGStab* with the stopping criterion as $\|r_i\|_2 / \|r_0\|_2 \leq tol$ for $tol = 10^{-7}$ (r_i is the residual of the corresponding system at the i^{th} iteration) applied to the unpermuted system and Schur complement system with and without preconditioning on the finest levels of uniformly (4^{th} refinement level with dof 196608 and 32768 triangular elements) and adaptively (17^{th} refinement level with dof 70716 and 11786 triangular elements) refined meshes. As a preconditioner, the incomplete LU factorization of the Schur complement matrix S ($ILU(S)$) is used for the linear system with the coefficient matrix S . The linear systems with the coefficient matrix A are solved directly. Table 1 shows that solving the problem via the block LU factorization using the Schur complement system with the preconditioner $ILU(S)$ is the fastest.

Linear Solver	# Newton	# BiCGStab	Time
BiCGStab w/o prec. (Unpermuted)	10.8 (10.5)	818 (757.5)	1389.3 (773.3)
BiCGStab w/ prec. M_1 (Permuted)	10.3 (10.3)	1.5 (3)	423.1 (374.2)
BiCGStab w/ prec. M_2 (Permuted)	10.3 (10.3)	1.5 (3)	416.8 (375.9)
Block LU + (BiCGStab w/o prec.)	10.3 (10.9)	247.5 (315.5)	270.9 (310.3)
Block LU + (BiCGStab w/ prec. $ilu(S)$)	10.3 (10.9)	19 (28.5)	140.9 (114.7)

Table 1: Example 6.1: Average number of Newton iterations, average number of *BiCGStab* iterations, total computation time in seconds corresponding to the uniformly refined (adaptively refined) mesh.

The time for applying the permutation to obtain the reordered matrix and the permutation matrix P takes 9.9 seconds, whereas, it takes 0.13 seconds to form the Schur complement matrix S and 0.04 seconds to compute the $ILU(S)$ on a PC with Intel Core-i7 processor and 8GB RAM using the 64-bit version of Matlab-R2010a. We note that since the Jacobian matrix does

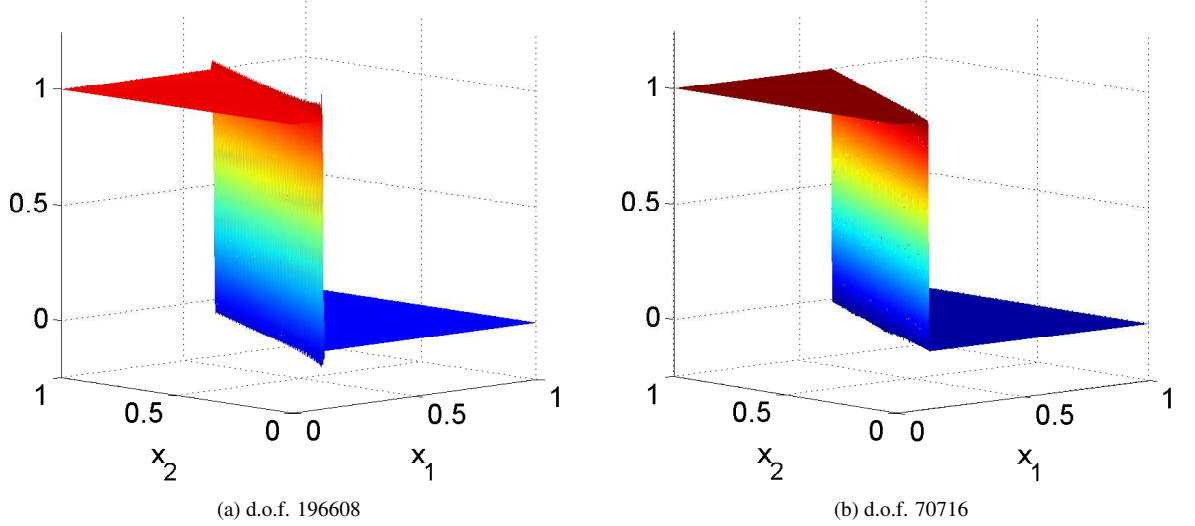


Figure 11: Example 6.1: Uniform(left) and adaptive(right) solutions, quadratic elements.

not change during the non-linear iterations, the permutation, the Schur complement matrix and $ILU(S)$ is computed only once for each run.

In all of the following results and figures, the Jacobian matrix J is scaled by a left Jacobi preconditioner before reordering to obtain a well conditioned matrix. The reordering procedure is applied to the scaled Jacobian matrix. Reordering times, which are included in the total computation time, for the uniform and adaptive refinements are 102.1 seconds and 41.4 seconds, respectively.

Fig.15 shows the condition numbers of the Jacobian matrices J of the original system, S and A of the block LU factorized system on the uniformly and adaptively refined meshes. The condition numbers of the coefficient matrix A are almost constant for uniform refinement by different orders of DG discretizations and around 10, whereas the condition number of S lower than of the Jacobian matrix J . This is due to the clustering of nonzero elements around the diagonal (Fig.16) due to the matrix reordering. For adaptive refinement, Fig.15, bottom, we observe the same behavior, whereas the conditions numbers are larger of order one than for the uniform refinement. For comparison, we provide results by using BiCGStab with two block preconditioners. The preconditioning matrices M_1 and M_2 for the permuted full systems are given as

$$M_1 = \begin{pmatrix} A & 0 \\ C^T & S \end{pmatrix}, \quad M_2 = \begin{pmatrix} A & B \\ 0 & S \end{pmatrix}.$$

Total number of iterations and time for different algorithms are given in Table 1. Our proposed method where we compute the block LU factorization of the partitioned matrix and solve the system involving the Schur complement iteratively via preconditioned BiCGStab is the best in terms of the total time compared to other methods for both uniform and adaptive refinement. In Fig.13 and Fig.14, we present the total time and the average number of linear solver iterations,

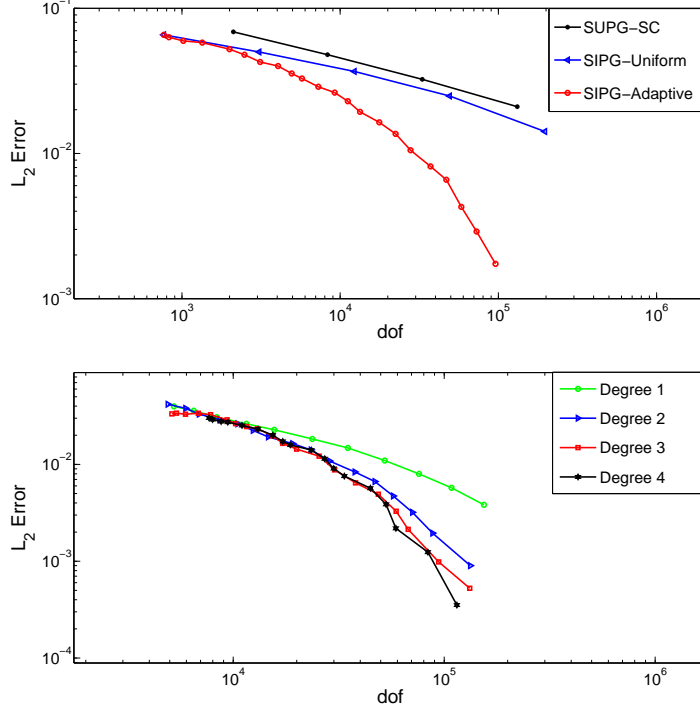


Figure 12: Example 6.1: Global errors: comparison of the methods by quadratic elements(top), adaptive DG for polynomial degrees 1-4(bottom).

respectively, for uniform and adaptive refinements as the problem size has been increased. We observe that the proposed preconditioned linear solver has been the best in terms of time with a reasonable number of iterations for different problem sizes regardless refinement type.

6.2. Example with Monod type non-linearity

We consider the Monod type non-linearity in (Bause, 2010):

$$u - \nabla \cdot (\epsilon \nabla u) + \mathbf{b} \cdot \nabla u - \frac{u}{1+u} = f$$

on $\Omega = (0, 1)^2$ with the convection field $\mathbf{b}(x_1, x_2) = (-x_2, x_1)^T$, diffusion coefficient $\epsilon = 10^{-6}$ and the source function $f = 0$. The Dirichlet boundary is prescribed as $u(x_1, x_2) = 1$ for $1/3 \leq x_1 \leq 2/3, x_2 = 0$ and $u(x_1, x_2) = 0$ on the remaining parts of the lower boundary as well as on the right and upper boundary. Moreover, $\frac{\partial u(x_1, x_2)}{\partial \mathbf{n}} = 0$ for $x_1 = 0, 0 \leq x_2 \leq 1$ where \mathbf{n} is the outer unit normal.

There are both internal and boundary layers on the mesh (Fig.17, left), around them oscillations occur. Fig.17, right, shows that by DGAFEM, the oscillations are almost disappear, similar to the results in (Bause, 2010) for the SUPG-SC and in (Yücel et al., 2013) for SIPG-SC. Fig.17, left, shows that the adaptive process leads to correctly refined meshes. Moreover, by increasing polynomial degree of the basis functions ($k = 4$), the oscillations are completely eliminated on

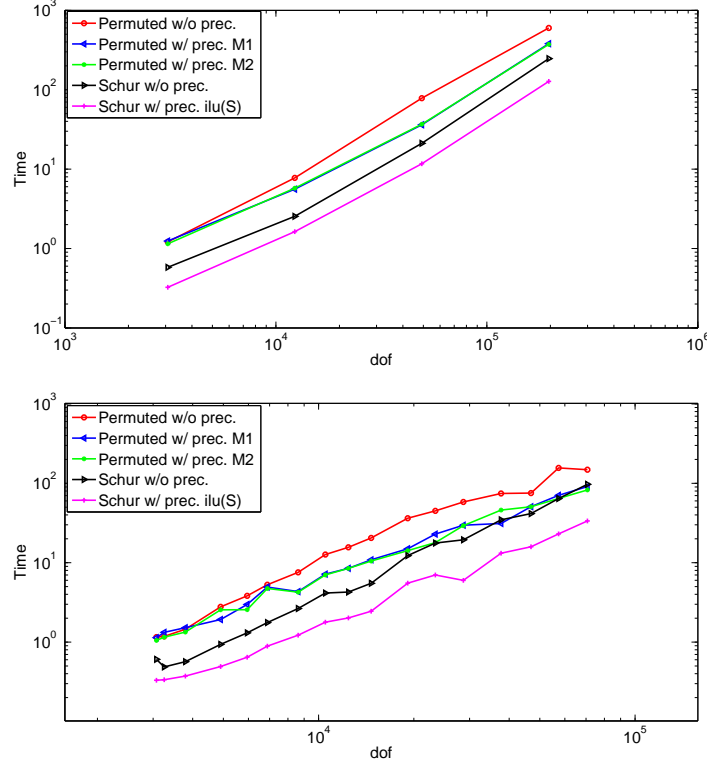


Figure 13: Example 6.1: Computation time vs. dof: Uniform refinement (top) and adaptive refinement (bottom)

the outflow boundary (Fig.17, bottom) and the sharp front is preserved. This is not the case for SUPG-SC (Bause, 2010) and SIPG-SC (Yücel et al., 2013), where still small oscillations are present.

As in case of polynomial non-linearity, Example 5.1, the block LU factorized system solved by BiCGStab with the preconditioner ILU(S) is the most efficient solver, with an average number of 7 Newton iterations. The computing times for the uniform refinement was 20.6 seconds, and 30.5 for the adaptive refinement.

6.3. Example with Arrhenius type non-linearity

Next example is the non-linear reaction for a two-component system in (Tezduyar & Park, 1986):

$$\begin{aligned} -\nabla \cdot (\epsilon \nabla u_1) + \mathbf{b} \cdot \nabla u_1 - 100k_0 u_2 e^{\frac{-E}{Ru_1}} &= 0, \\ -\nabla \cdot (\epsilon \nabla u_2) + \mathbf{b} \cdot \nabla u_2 + k_0 u_2 e^{\frac{-E}{Ru_1}} &= 0 \end{aligned}$$

on $\Omega = (0, 1)^2$ with the convection field $\mathbf{b} = (1 - x_2^2, 0)^T$, the diffusion constant $\epsilon = 10^{-6}$, the reaction rate coefficient $k_0 = 3 \times 10^8$ and the quotient of the activation energy to the gas constant

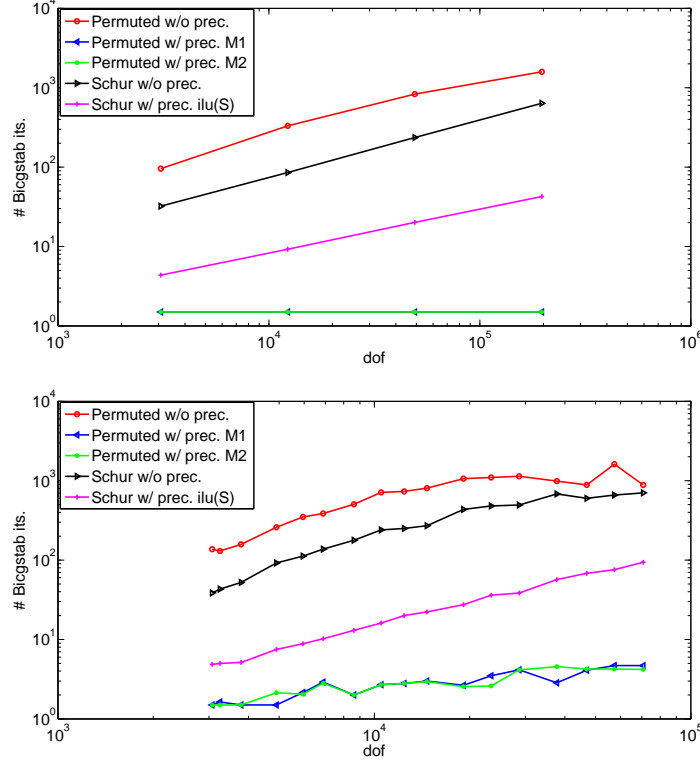


Figure 14: Example 6.1: # Average *BiCGStab* iterations vs. dof: Uniform refinement (top) and adaptive refinement (bottom)

$\frac{E}{R} = 10^4$. The unknowns u_1 and u_2 represent the temperature of the system and the concentration of the reactant, respectively.

There are oscillations around the layers, even small, for the uniform refinement (Fig.18, left) as for SIPG-SC in (Yücel et al., 2013). On the other hand, these oscillations are completely dumped out by DGAFEM with almost half of the dof used in the uniform refinement (Fig.18, right).

The block LU factorization based algorithm with the preconditioner ILU(S) requires 10.5 seconds for the uniform and 24.4 seconds for the adaptive refinements. Matrix reordering and permutation took 2.44 seconds for the uniform and 2.17 seconds for adaptive refinements, respectively.

6.4. Coupled example with polynomial type non-linearity

Our final problem is the modification of the non-stationary transport problem, Example 2, in (Bause & Schwegler, 2013). The problem is stated as the following:

$$\begin{aligned} \alpha u_1 - \nabla \cdot (\epsilon \nabla u_1) + \mathbf{b} \cdot \nabla u_1 + 50u_1^2 u_2^2 &= 0, \\ \alpha u_2 - \nabla \cdot (\epsilon \nabla u_2) + \mathbf{b} \cdot \nabla u_2 + 50u_1^2 u_2^2 &= 0 \end{aligned}$$

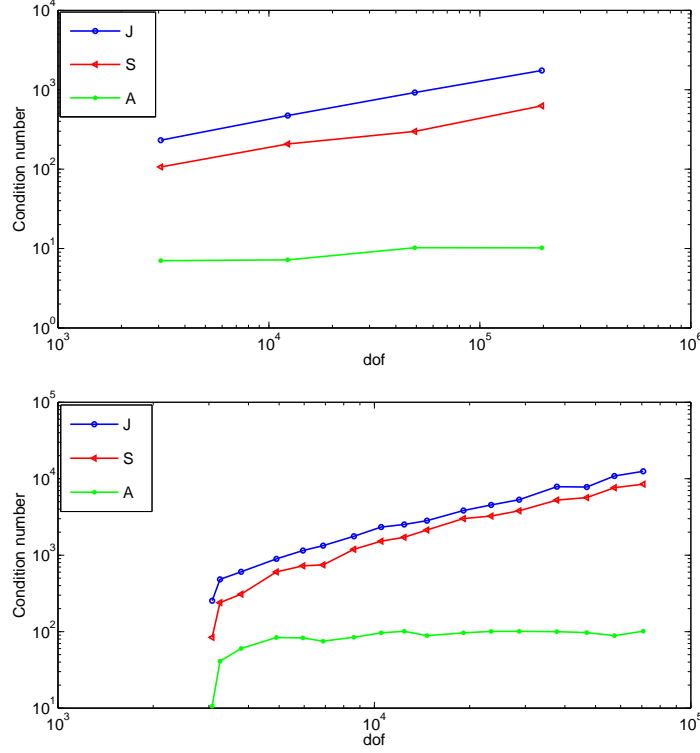


Figure 15: Example 6.1: Condition number of the matrices J (unpermuted matrix), S (Schur complement matrix) and A (left top block of permuted matrix): Uniform refinement (top) and adaptive refinement (bottom).

on the rectangular domain $\Omega = (0, 1) \times (0, 2)$ with the convection field $\mathbf{b} = (0, -1)^T$, the diffusion constant $\epsilon = 10^{-10}$ and linear reaction constant $\alpha = 0.1$. On the left, right and lower parts of the boundary of the domain, Neumann boundary conditions are prescribed. On the remaining part of the boundary, Dirichlet boundary conditions are chosen as

$$u_1(\mathbf{x}) = \begin{cases} 8(x_1 - 0.375) & \text{for } 0.375 < x_1 \leq 0.5, \\ -8(x_1 - 0.625) & \text{for } 0.5 < x_1 \leq 0.625, \\ 0 & \text{otherwise} \end{cases}$$

$$u_2(\mathbf{x}) = \begin{cases} 8(x_1 - 0.125) & \text{for } 0.125 \leq x_1 \leq 0.25, \\ -8(x_1 - 0.375) & \text{for } 0.25 < x_1 \leq 0.375, \\ 8(x_1 - 0.625) & \text{for } 0.625 \leq x_1 \leq 0.75, \\ -8(x_1 - 0.875) & \text{for } 0.75 < x_1 \leq 0.875, \\ 0 & \text{otherwise} \end{cases}$$

There is a boundary layer on the outflow boundary, Fig.20. Fig.19 shows that oscillations are almost damped using DGAFEM approximations, similar to those results in (Bause & Schwegler,

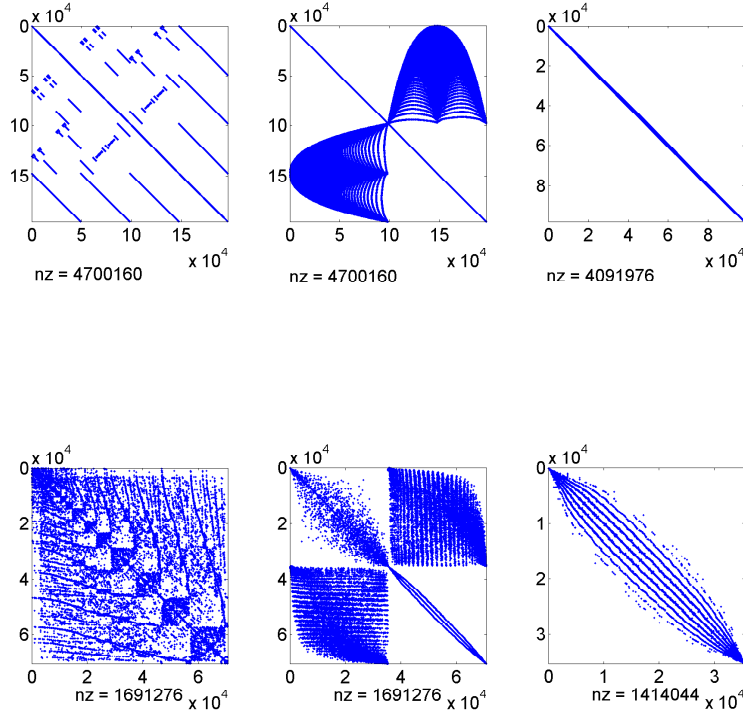


Figure 16: Example 6.1: Sparsity patterns of the unpermuted (left), permuted (middle) and the Schur complement (right) matrices at the final refinement levels: Uniform refinement (top) with dof 196608 and adaptive refinement (bottom) with dof 70716.

2013) using SUPG-SC. It can be seen from Fig.20 that the mesh is correctly refined by DGAFEM near the boundary layer.

7. Conclusions

We have shown that using DGAFEM with the sparse linear solver is an efficient method for solving non-linear convection dominated problems accurately and avoids the design of the parameters in the shock capturing technique as for the SUPG-SC and DG-SC methods. The numerical examples demonstrate that DGAFEM allows to capture the interior and boundary layers very sharply without any significant oscillation. As a future study, we will apply space-time adaptive DG methods for time-dependent convection dominated non-linear diffusion-convection-reaction equations.

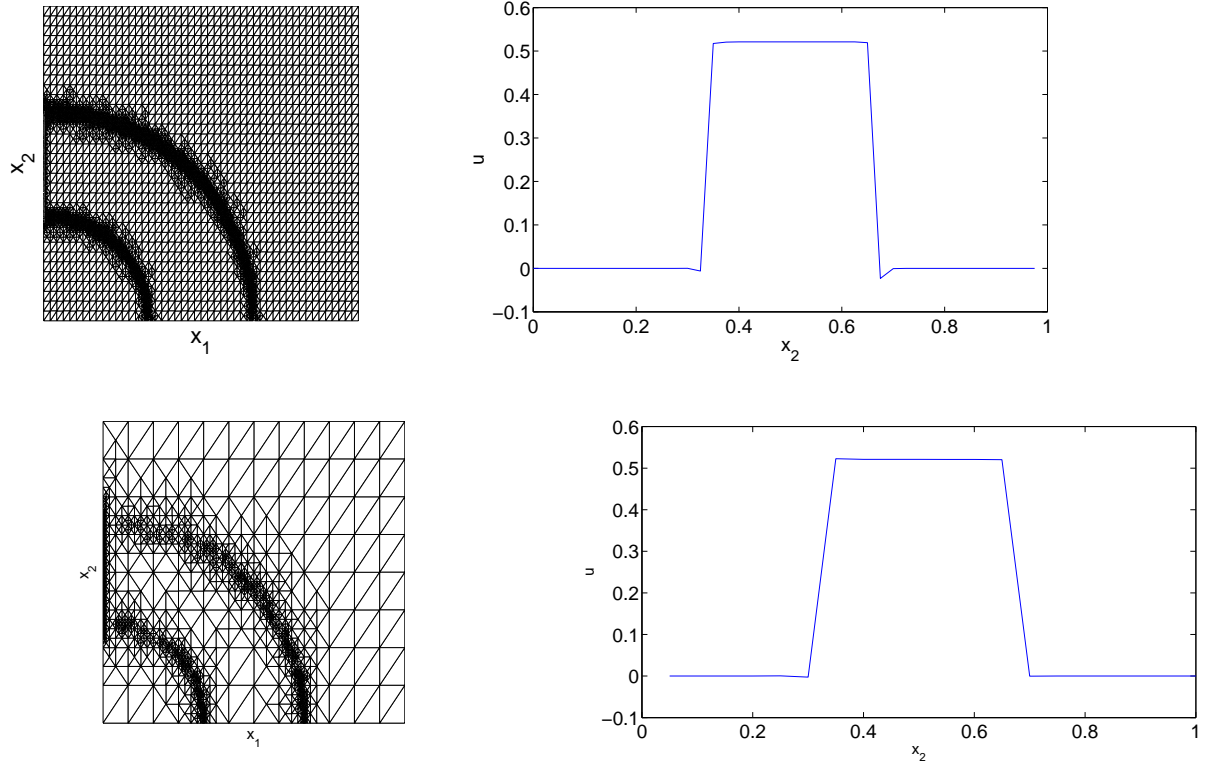


Figure 17: Example 6.2: Adaptive meshes (left) and the cross-section plots (right) of the solutions at the left outflow boundary by quadratic elements (top) with dof 82464 and quartic elements (bottom) with dof 80530

Acknowledgment

The authors would like to thank the reviewer for the comments and suggestion that help improve the manuscript. This work has been partially supported by Turkish Academy of Sciences Distinguished Young Scientist Award TUBA-GEBIP/2012-19, TÜBİTAK Career Award EEAG111E238 and METU BAP-07-05-2013-004.

References

- Antonietti, P. F., Süli, E. (2009). Domain decomposition preconditioning for discontinuous Galerkin approximations of convection-diffusion problems. *Domain Decomposition Methods in Science and Engineering XVIII*, eds. M. Bercovier, M. J. Gander, R. Kornhuber, O. Widlund, *Lecture Notes in Computational Science and Engineering*, Volume 70, 259-266.
- Arnold, D., Brezzi, F., Cockburn, B., & Marini, L. (2002). Unified analysis of discontinuous Galerkin methods for elliptic problems. *SIAM J. Numer. Anal.*, 39, 1749-1779.
- Ayuso, B., & Marini, L.D. (2009). Discontinuous Galerkin methods for advection-diffusion-reaction problems. *SIAM J. Numer. Anal.*, 47, 1391-1420.

- Barnard, S.T., Pothen, A., & Simon, H. (1995). A spectral algorithm for envelope reduction of sparse matrices. *Numerical linear algebra with applications*, 4, 317-334.
- Bause, M. (2010). Stabilized finite element methods with shock-capturing for non-linear convection-diffusion-reaction models. In *Numerical Mathematics and Advanced Applications 2009*, 125-134. Springer Berlin Heidelberg.
- Bause, M., & Schwegler, K. (2012). Analysis of stabilized higher-order finite element approximation of nonstationary and non-linear convection-diffusion-reaction equations. *Comput. Methods Appl. Mech. Engrg.*, 209-212 184-196.
- Bause, M., & Schwegler, K. (2013). Higher order finite element approximation of systems of convectiondiffusionreaction equations with small diffusion. *Journal of Computational and Applied Mathematics*, 246, 52-64.
- Benzi, M., Golub, G.H., & Liesen, J. (2005). Numerical solution of saddle point problems. *Acta numerica*, 14, 1-137.
- Bochev, P.B., & Gunzburger, M.D. (1998). Finite element methods of least-squares type. *SIAM Review*, 40, 789-837.
- Bochev, P.B., & Gunzburger, M.D. (2009). Least-squares finite element methods. *Applied Mathematical Sciences*, 166. Springer.
- Brooks, A.N., & Hughes, T.J.R. (1982). Streamline upwind/Petrov-Galerkin formulations for convection dominated flows with particular emphasis on the incompressible Navier/Stokes equations. *Comp. Meth. Appl. Mech. Eng.*, 32, 199-259.
- Cangiani, A., Chapman, J., Georgoulis, E., & Jensen, M. (2013). On the Stability of Continuous of Discontinuous Galerkin Methods for Advection-Diffusion-Reaction Problems. *J. Journal of Scientific Computing*, 57, 313-330.
- Castillo, P. (2012). Performance of discontinuous Galerkin methods for elliptic PDEs. *SIAM J. Sci. Comput.*, 24, 524-547.
- Chen, L. (2008). iFEM: an innovative finite element method package in MATLAB, an innovative finite element methods package in MATLAB. *Tech. rep.:Department of Mathematics, University of California, Irvine*.
- Deng, S., & Cai, W. (2005). Analysis and Application of an Orthogonal Nodal Basis on Triangles for Discontinuous Spectral Element Methods. *Appl. Num. Anal. Comp. Math*, 2, 326-345.
- Dobrev, V.A., Lazarov, R.D., & Zikatanov, L.T. (2008). Preconditioning of symmetric interior penalty discontinuous Galerkin FEM for elliptic problems. In: *Domain Decomposition Methods in Science and Engineering XVII, Lecture Notes in Computer Science and Engineering*, 60, 3344. Springer.
- Dörfler, W. (1996). A convergent adaptive algorithm for Poissons equations. *SIAM Journal on Numerical Analysis*, 33:1106-1124.
- Dolejší, V. (2008). Analysis and application of IIPG method to quasilinear nonstationary convection-diffusion problems. *J. Comp. Appl. Math.*, 222, 251-273.
- Dolejš, V., Feistauer, M., & Sobotiková, V. (2005). Analysis of the discontinuous Galerkin method for non-linear convection diffusion problems. *Comput. Methods Appl. Mech. Eng.*, 194, 2709-2733.
- Dolejší, V. (2013). hp-DGFEM for non-linear convection-diffusion problems. *Mathematics and Computers in Simulation*, 87, 87-118.
- Epshteyn, Y., & Riviere, B. (2007). Estimation of penalty parameters for symmetric interior penalty Galerkin methods. *J. Comput. Appl. Math.*, 206, 843-872.
- Fiedler, M. (1973). Algebraic connectivity of graphs. *Czechoslovak Mathematical Journal*, 23, 298-305.
- Fiedler, M. (1975). A property of eigenvectors of nonnegative symmetric matrices and its application to graph theory. *Czechoslovak Mathematical Journal*, 25, 619-633.
- Georgoulis, E., Loghin, D. (2008). Norm preconditioners for discontinuous Galerkin hp-finite element methods. *SIAM Journal on Scientific Computing*, 30, 2447-2465.
- G.Hauke, G. (2002). A simple subgrid scale stabilized method for the advection-diffusion-reaction equation. *Comput. Methods. in Applied Mech. and Eng.*, 191, 2925-2947.
- Hoppe, R.H.W., Kanschat, G., & Warburton, T. (2008). Convergence analysis of an adaptive interior penalty discontinuous Galerkin method. *SIAM Journal on Numerical Analysis*, 47,534-550.
- Houston, P., Schwab, C., & Süli, E. (2002). Discontinuous hp-finite element methods for advection-diffusion-reaction problems. *SIAM J. Numer. Anal.*, 39, 2133-2163.
- Houston, P., Jensen, M., & Süli, E. (2002). hp-discontinuous Galerkin finite element methods with least-squares stabilization. *J. Sci. Comput.*, 17, 3-25.
- Hughes, T.J.R., Franca, L.P. & Hulbert, G.M. (1989). A new finite element formulation for fluid dynamics:viii. The Galerkin/least-squares method for the advection-diffusion equations. *Comput. Methods Appl. Mech. Engrg.*, 73, 173-189.
- Jiang, B.N. (1998). The Least-squares Finite Element Method. Theory and Applications in Computational Fluid Dynamics and Electromagnetics. Springer.
- R.D. Lazarov and P.S. Vassilevski (2000). Least-squares streamline diffusion finite element approximations to singularly perturbed convection-diffusion problems. *Analytical and Numerical Methods for Singularly Perturbed Problems*, (L.G. Vulkov, J.J.H. Miller, and G.I. Shishkin, Eds.), Nova Science Publishing House, 83-94.
- Manguoğlu, M., Koyutürk, M., Sameh, A.H., & Grama, A. (2010). Weighted matrix ordering and parallel banded preconditioners for iterative linear system solvers. *SIAM Journal on Scientific Computing*, 32, 1201-1216.
- Persson, P., & Peraire, J. (2006). Sub-cell shock capturing for discontinuous galerkin methods. In *Proc. of the 44th AIAA*

- Aerospace Sciences Meeting and Exhibit*, volume 112.
- Rivière, B. (2008). *Discontinuous Galerkin methods for solving elliptic and parabolic equations. Theory and implementation*, SIAM.
- Schötzau, D., & Zhu, L. (2009). A robust a-posteriori error estimator for discontinuous Galerkin methods for convection-diffusion equations. *Applied Numerical Mathematics*, 59, 2236-2255.
- Slingerland, P., & Vuik, C. (2014). Fast linear solver for diffusion problems with applications to pressure computation in layered domains, *J Computational Geosciences*, to appear.
- Solsvik, J., Tangen, S., & Jakobsen, H. A. (2013). Evaluation of weighted residual methods for the solution of the pellet equations: The orthogonal collocation, Galerkin, tau and least-squares methods. *Computers and Chemical Engineering*, 58, 223–259.
- Tari, O., & Manguoğlu, M. (2013). Revealing the Saddle Point Structure Using the Largest Eigenvector of the Laplacian. *International Conference On Preconditioning Techniques For Scientific And Industrial Applications* (19-21 June 2013), Oxford, UK.
- Tezduyar, T.E., & Park, Y.J. (1986). Discontinuity-capturing finite element formulations for non-linear convection-diffusion-reaction equations. *Computer Methods in Applied Mechanics and Engineering*, 59, 307-325.
- Verfürth, R. (2013). *A posteriori Error Estimates Techniques for Finite Element Methods*. Oxford University Press.
- Yücel, H., Heinkenschloss, M., & Karasözen, B. (2013). Distributed optimal control of diffusion-convection-reaction equations using discontinuous Galerkin methods, in: A. Cangiani, R. Davidchack, E. Georgoulis, A. Gorban, J. Levesley, M. Tretyakov (eds.), *Numerical Mathematics And Advanced Applications. ENUMATH 2011*, 398-397. Springer, Heidelberg.
- Yücel, H., Stoll, M., & Benner, P. (2013). Discontinuous Galerkin finite element methods with shock-capturing for non-linear convection dominated models. *Computers and Chemical Engineering*, 58, 278-287.

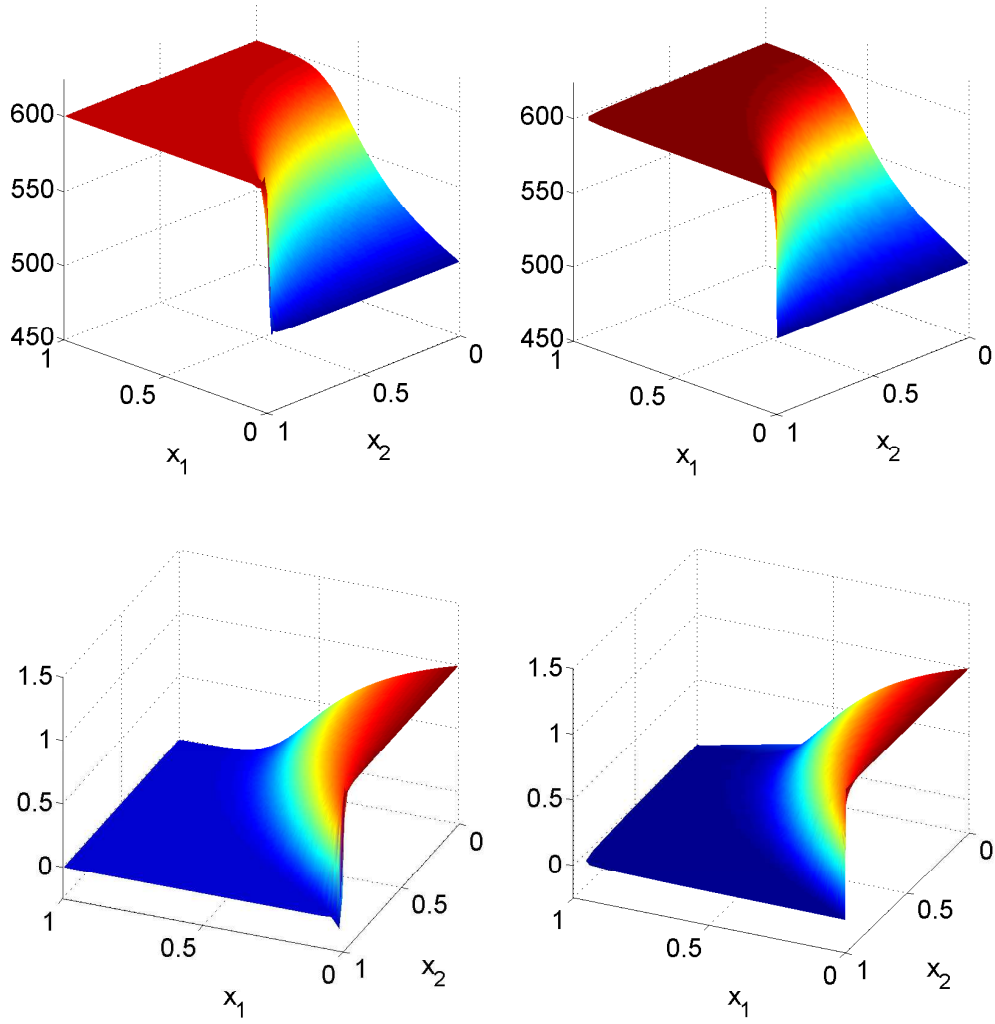


Figure 18: Example 6.3: Uniform(left) and adaptive(right) solutions to the temperature(top) and reactant(bottom), quadratic elements with dof 12288 for uniform refinement and with dof 6168 for adaptive refinement

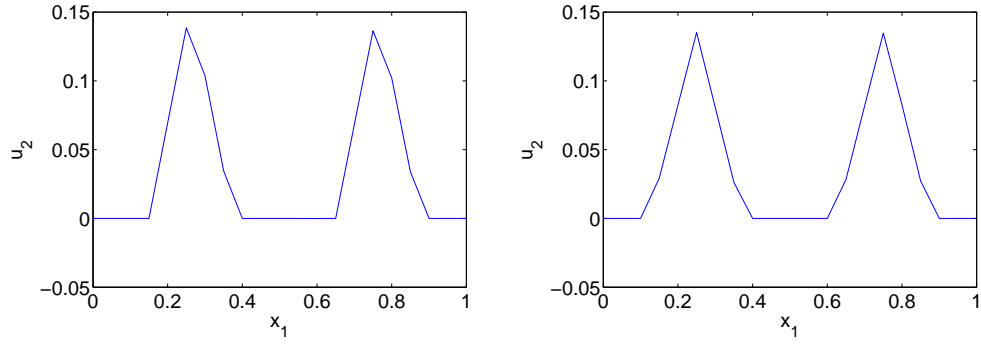


Figure 19: Example 6.4: Uniformly(left) and adaptively(right) obtained cross-section plots on the outflow boundary for the component u_2 , quartic elements with dof 61440 for uniform refinement and with dof 33690 for adaptive refinement.

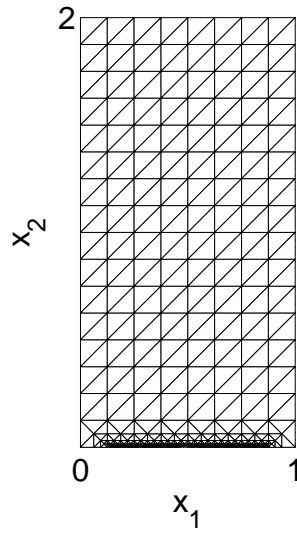


Figure 20: Example 6.4: Adaptive mesh, quartic elements with dof 33690.